



2017

Metal Chalcogenide Clusters with Closed Electronic Shells and the Electronic Properties of Alkalis and Halogens

Vikas Chauhan

Virginia Commonwealth University

Arthur C. Reber

Virginia Commonwealth University, acreber@vcu.edu

Shiv N. Khanna

Virginia Commonwealth University, snkhanna@vcu.edu

Follow this and additional works at: http://scholarscompass.vcu.edu/phys_pubs

 Part of the [Physics Commons](#)

© 2017 American Chemical Society

Downloaded from

http://scholarscompass.vcu.edu/phys_pubs/210

This Article is brought to you for free and open access by the Dept. of Physics at VCU Scholars Compass. It has been accepted for inclusion in Physics Publications by an authorized administrator of VCU Scholars Compass. For more information, please contact libcompass@vcu.edu.

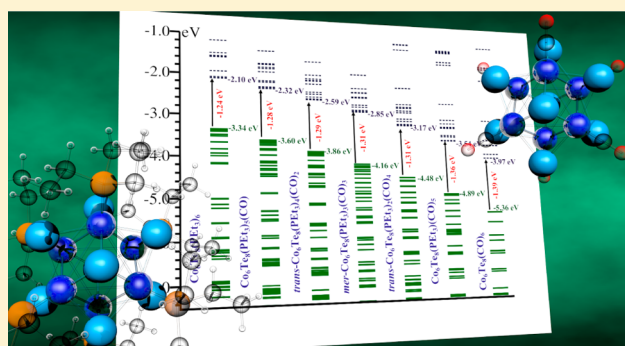
Metal Chalcogenide Clusters with Closed Electronic Shells and the Electronic Properties of Alkalis and Halogens

Vikas Chauhan, Arthur C. Reber, and Shiv N. Khanna*[✉]

Department of Physics, Virginia Commonwealth University, Richmond, Virginia, United States

S Supporting Information

ABSTRACT: Clusters with filled electronic shells and a large gap between the highest occupied molecular orbital (HOMO) and the lowest unoccupied molecular orbital (LUMO) are generally energetically and chemically stable. Enabling clusters to become electron donors with low ionization energies or electron acceptors with high electron affinities usually requires changing the valence electron count. Here we demonstrate that a metal cluster may be transformed from an electron donor to an acceptor by exchanging ligands while the neutral form of the clusters has closed electronic shells. Our studies on $\text{Co}_6\text{Te}_8(\text{PET}_3)_m(\text{CO})_n$ ($m + n = 6$) clusters show that $\text{Co}_6\text{Te}_8(\text{PET}_3)_6$ has a closed electronic shell and a low ionization energy of 4.74 eV, and the successive replacement of PET_3 by CO ligands ends with $\text{Co}_6\text{Te}_8(\text{CO})_6$ exhibiting halogen-like behavior. Both the low ionization energy $\text{Co}_6\text{Te}_8(\text{PET}_3)_6$ and high electron affinity $\text{Co}_6\text{Te}_8(\text{CO})_6$ have closed electronic shells marked by high HOMO–LUMO gaps of 1.24 and 1.39 eV, respectively. Further, the clusters with an even number of ligands favor a symmetrical placement of ligands around the metal core.



INTRODUCTION

Due to quantum confinement, the electronic states in compact clusters are bunched into electronic shells much like those in atoms leading to the proposition that clusters could be viewed as superatoms.^{1,2} Clusters with filled electronic shells and a large HOMO–LUMO gap are generally energetically stable and chemically inert and are often referred to as having “magic numbers”.^{3,4} Like atoms, superatoms with electron counts that are one past the filled shell exhibit low ionization energies, while those with a count that is deficient by one electron from the filled shell exhibit large electron affinities.^{5–10} These characteristics are rooted in the fact that an electron occupation past the filled shell leads to an electron occupying a high energy state, and removing the electron forms a highly stable cation causing a low ionization energy. Clusters that need an electron to acquire filled electronic shells form highly stable anions with closed electronic shell and a high electron affinity. This universal rule lies at the heart of the three-dimensional periodic table, and tuning the electron count is the conventional approach to creating clusters with low ionization energy or large electron affinity. One strategy to accomplish this is to use ligands that bond with the surface atoms to change the free electron count. In fact, over the past few years, a large number of solids based on stable ligated gold, silver, platinum, and aluminum clusters have been synthesized where the ligated clusters are frequently arranged in a crystalline form.^{11–25} The stability of the ligated clusters is generally rationalized within the superatomic picture where the ligands form covalent bonds that change the effective valence count of the metal core.²⁴

Stable species are formed as the valence count attains a value corresponding to a filled valence shell with a large HOMO–LUMO gap resembling noble gas atoms.

Roy, Nuckolls, and co-workers have recently proposed a new class of cluster assembled materials formed from metal chalcogenide clusters capped by various ligands.^{25–30} These highly stable building blocks can be prepared in solutions and have charge donor/acceptor characteristics, and can form either unary solids or binary solids with complementary units maintaining the identity of the internal structure. Nuckolls and co-workers have classified these clusters as superatoms in that the clusters are highly stable and offer a definite valence much like conventional superatoms. These clusters are marked by covalent bonds between transition metal d-states and the chalcogen p-states and therefore do not have the same shell structure as a confined nearly free electron gas. Their classification as superatoms therefore requires modification of the current superatomic framework, and in the remainder of this paper, we will refer to these as stable clusters. This class of clusters includes $\text{Co}_6\text{Se}_8(\text{PET}_3)_6$, $\text{Cr}_6\text{Te}_8(\text{PET}_3)_6$, and $\text{Ni}_9\text{Te}_6(\text{PET}_3)_8$ where metal-chalcogenide cores are decorated with triethylphosphine (PET_3) ligands attached to metal sites.^{31–39} These clusters are found to be quite stable and form ordered ionic compounds when combined with C_{60} where the clusters act as electron donors with C_{60} having a high electron affinity as an acceptor.²⁵ Theoretical studies indicate

Received: September 7, 2016

Published: January 12, 2017

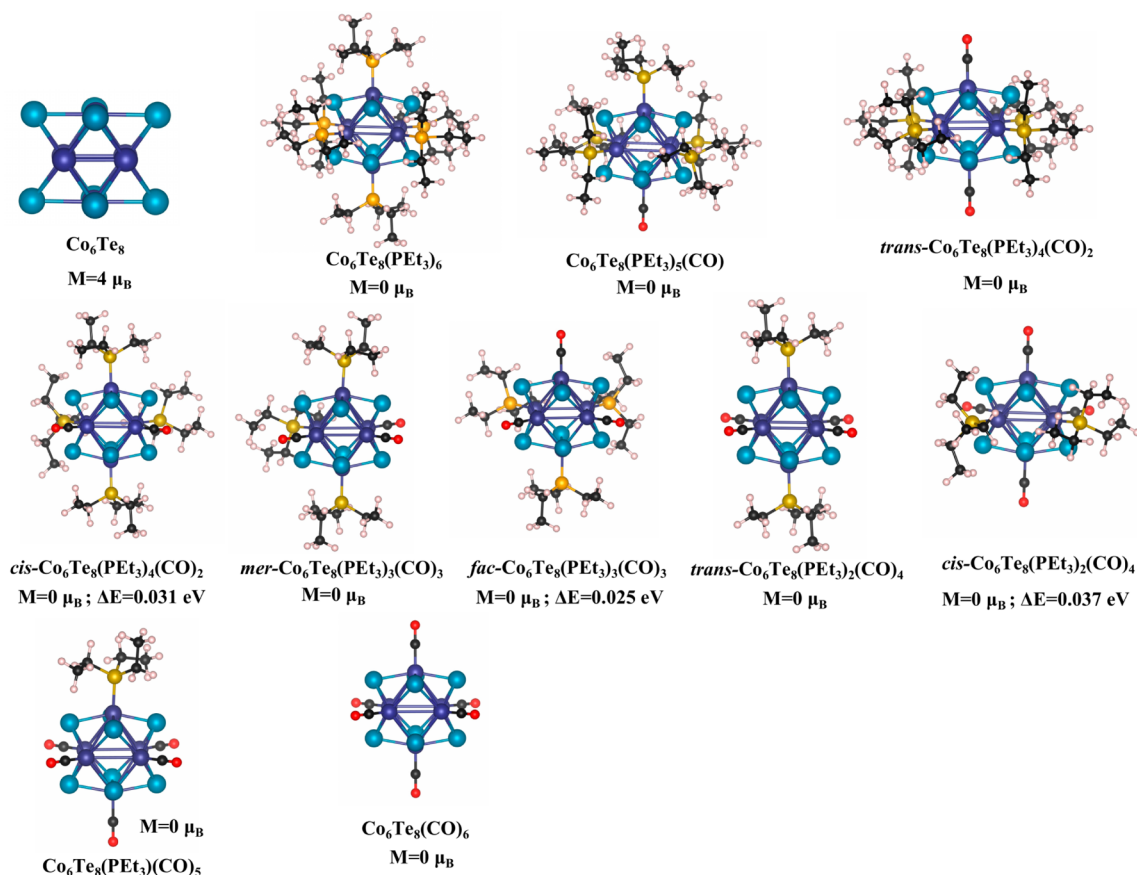


Figure 1. Optimized ground state structures of a bare Co_6Te_8 and ligated $\text{Co}_6\text{Te}_8(\text{PEt}_3)_m(\text{CO})_n$ ($m + n = 6$) clusters. The Co, Te, P, C, H, and O atoms are represented by dark blue, cyan blue, orange, black, white, and red colors, respectively. Magnetic moments in the ground state are also given.

that the phosphine ligands bind to the cluster motif by forming charge transfer complexes.³⁴ More recent studies have focused on manipulating metal–ligand bonds to create motifs offering newer features. This includes replacing electron donor PEt_3 ligands by electron acceptor CO ligands or isonitriles to form their dimers.^{29,34} One of the fundamental issues is how the metal–ligand bonding can be used to control the cluster properties.

The purpose of this paper is to propose that the ligand manipulation can be used to transform a cluster from an electron acceptor to an electron donor without changing the effective valence count. We will study neutral clusters that have filled electronic shells yet find they may act as superb electron donors or acceptors forming a new class of donor/acceptors.⁴⁰ We illustrate this by considering a $\text{Co}_6\text{Te}_8(\text{PEt}_3)_6$ cluster that has a closed electronic shell with a high HOMO–LUMO gap of 1.24 eV. This cluster has a low ionization energy and a low electron affinity. Replacement of PEt_3 ligands by CO is shown to monotonically increase the ionization energy from 4.91 to 7.03 eV for $\text{Co}_6\text{Te}_8(\text{CO})_6$. The increase in ionization energy is followed by an increase in the electronic affinity from 1.19 eV for $\text{Co}_6\text{Te}_8(\text{PEt}_3)_6$ to 2.60 eV for $\text{Co}_6\text{Te}_8(\text{CO})_6$. The unusual feature is that, irrespective of the combination of ligands, the ligated species always have a closed shell electronic configuration with a high HOMO–LUMO gap varying from 1.24 to 1.39 eV. By changing the ligand, the polarity of the interaction between the Co 4s orbital and the lone pair of the ligand changes, but the effective valence electron count remains the same. The change in the electronic character is not

associated with a change in the electron count but due to a shift in the electronic spectrum that can be rationalized as ligands forming a coulomb well that surrounds the cluster and may raise or lower the energy of the states depending on the donor–acceptor characteristics of the ligand. The ability to stabilize the different charged states is not only crucial for forming solids with different classes of counterions (donors or acceptors) but also in photovoltaic applications requiring control over oxidation states.^{41–43}

METHODS

First-principles theoretical studies were carried out using the Amsterdam density functional (ADF) set of codes.⁴⁴ The generalized gradient approximation (GGA) functional proposed by Perdew, Burke, and Ernzerhof (PBE) was used to include the exchange and correlation effect.⁴⁵ The Slater-type orbitals (STOs) located at the atomic sites are used to express the atomic wave function, while the cluster wave functions are built from a linear combination of these atomic orbitals. A TZ2P basis set and a large frozen electron core are used. For mixed ligands, numerous structures corresponding to various positions of ligands were examined. The total energies and the forces at the atomic sites are computed, and a quasi-Newton method without any symmetry restriction is applied to find out the local minimum for each structure. Scalar-relativistic effects were included via zero-order regular approximation (ZORA).⁴⁶ The calculations are carried out over neutral, anionic, and cationic species, and several possible spin multiplicities were considered for all clusters.

RESULTS AND DISCUSSION

Figure 1 shows the ground state structure of the ligand-free Co_6Te_8 cluster. It corresponds to an octahedron of Co atoms with eight triangular faces decorated by Te atoms. The Co–Co bond lengths vary between 2.53 and 2.57 Å and are almost the same as in bulk Co, whereas the Co–Te bonds are 2.54–2.55 Å. The ligand-free cluster has a spin magnetic moment of 4.0 μ_B , and an analysis of the spin density shows that the spin magnetic moments on Co atoms (4.983 μ_B) are aligned antiparallel to that of Te atoms (–0.983 μ_B). We have also calculated the adiabatic ionization energy (AIE) and adiabatic electron affinity (AEA) using the total energy difference between the ground states of neutral and corresponding cation and anion, respectively. It has an adiabatic ionization energy of 6.33 eV and adiabatic electron affinity of 2.81 eV. We first examined the evolution of the electronic and magnetic properties as the chalcogenide core is ligated with PET_3 groups. The ligands attach to the Co sites, and hence, the cluster takes six PET_3 ligands. In the case of full ligation with PET_3 , Co–Co bond lengths increase and vary between 3.28 and 3.32 Å. The Co–Te and Co–P bond lengths are found to be 2.56 and 2.15 Å consistent with the corresponding experimental values of 2.52 and 2.13 Å, respectively.⁴⁷ The ligation both quenches the magnetic moment and increases the HOMO–LUMO gap to be 1.24–1.39 eV. This result is interesting in view of our recent studies on the effect of ligation on Ni_9Te_6 clusters that is also magnetic, and the attachment of PET_3 or CO ligands preserves the spin ground state of bare Ni_9Te_6 .³⁴ On the contrary, here PET_3 strongly reduces the magnetic character of Co_6Te_8 completely quenching the moment of bare Co_6Te_8 . The next spin isomer, i.e., triplet, is 0.89 eV higher in energy with respect to the ground state. Our findings are supported by the previous theoretical study of the ligated $\text{Co}_6\text{X}_8(\text{PET}_3)_6$ (X = S, Se, and Te) clusters reported by Bencini et al., who also find a nonmagnetic ground state.⁴⁸ A Mulliken spin density analysis indicates the absence of spin polarization at the Co sites confirming the absence of any local spin polarization. This is important, as an absence of net moment can also result from an antiferromagnetic alignment of spins. Furthermore, the AIE and AEA of $\text{Co}_6\text{Te}_8(\text{PET}_3)_6$ are found to be 4.75 and 1.19 eV, respectively. In fact, both the AIE and AEA were reduced from their value for Co_6Te_8 by around 1.6 eV, showing that the ligands are leading to a rigid shift in both of the electronic features. Another interesting effect is the change in the HOMO–LUMO gap, as the value for $\text{Co}_6\text{Te}_8(\text{PET}_3)_6$ is 1.24 eV compared to 0.16 eV for a bare Co_6Te_8 cluster. The one electron energy levels of Co_6Te_8 and $\text{Co}_6\text{Te}_8(\text{PET}_3)_6$ are shown in Figure SI-I. As mentioned earlier, our key objective is to examine the effect of ligand exchange on the electronic properties as PET_3 ligands are replaced by electron withdrawing CO ligands. Therefore, we also optimized the geometries of $\text{Co}_6\text{Te}_8(\text{PET}_3)_m(\text{CO})_{6-m}$ ($0 \leq m \leq 6$) as the PET_3 ligands were successively replaced by CO ligands. In each case, we examined various positions of the ligands and optimized the structure and spin multiplicities. The resulting ground state and low lying structures are shown in Figure 1. For two CO ligands, one can obtain a *trans* arrangement of $\text{Co}_6\text{Te}_8(\text{PET}_3)_4(\text{CO})_2$ where the ligands are attached to two Co atoms across from each other, while adjacent ligation results in a *cis* isomer shown in Figure 1. Attachment of one more CO in a row and a face of Co_6Te_8 results in *mer* and *fac* isomers of $\text{Co}_6\text{Te}_8(\text{PET}_3)_3(\text{CO})_3$. Subsequently, the fourth CO ligand leads again to a *trans* and

cis isomer of $\text{Co}_6\text{Te}_8(\text{PET}_3)_2(\text{CO})_4$. Our first-principles calculations predict the *trans* isomers of $\text{Co}_6\text{Te}_8(\text{PET}_3)_4(\text{CO})_2$ and $\text{Co}_6\text{Te}_8(\text{PET}_3)_2(\text{CO})_4$ to be the ground state, while corresponding *cis* isomers are 0.031 and 0.037 eV higher in energy, respectively. The *mer*- $\text{Co}_6\text{Te}_8(\text{PET}_3)_3(\text{CO})_3$ is found to be 0.025 eV lower in energy compared to *fac*- $\text{Co}_6\text{Te}_8(\text{PET}_3)_3(\text{CO})_3$. As the ligands are attached to the Co sites, they mainly perturb the Co–Co bond lengths. For example, Co–Co bond lengths in $\text{Co}_6\text{Te}_8(\text{CO})_6$ are found to be 3.16 Å, which are smaller than the corresponding values in $\text{Co}_6\text{Te}_8(\text{PET}_3)_6$. The Co–Te, Co–P, and Co–C bond lengths were found to be relatively unchanged regardless of the composition. All of the bond lengths of ligated clusters are provided in Table SI-I.

We next examined the binding energy of the PET_3 and CO ligands at different compositions to examine the feasibility of the replacement. To this end, we calculated the binding energy of PET_3 or CO from $\text{Co}_6\text{Te}_8(\text{L}_1)_m(\text{L}_2)_n$ clusters, where $\text{L}_1 = \text{PET}_3$, $\text{L}_2 = \text{CO}$, and $m + n = 5$. The ligand binding energies B.E. (L_1) and B.E. (L_2) were determined using eqs 1 and 2

$$\text{B.E.}(\text{L}_1) = E(\text{Co}_6\text{Te}_8(\text{L}_1)_{m-1}(\text{L}_2)_n) + E(\text{L}_1) - E(\text{Co}_6\text{Te}_8(\text{L}_1)_m(\text{L}_2)_n) \quad (1)$$

$$\text{B.E.}(\text{L}_2) = E(\text{Co}_6\text{Te}_8(\text{L}_1)_m(\text{L}_2)_{n-1}) + E(\text{L}_2) - E(\text{Co}_6\text{Te}_8(\text{L}_1)_m(\text{L}_2)_n) \quad (2)$$

where E is the total energy of the system. The calculated values are displayed in Figure 2. Note that, while the PET_3 binding

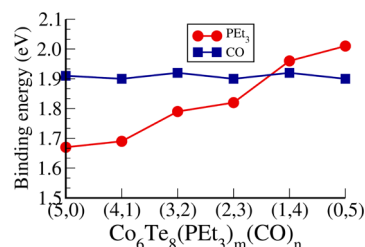


Figure 2. Binding energy of PET_3 and CO ligand from $\text{Co}_6\text{Te}_8(\text{PET}_3)_m(\text{CO})_n$ ($m + n = 5$) clusters.

energy varies between 1.69 and 2.01 eV, the energy to remove CO has a fairly constant value around 1.90 eV. Starting from the $\text{Co}_6\text{Te}_8(\text{PET}_3)_6$ cluster, it is energetically favorable to replace the first four PET_3 ligands by CO after which the attachment of PET_3 is more favorable, as the most stable cluster is $\text{Co}_6\text{Te}_8(\text{PET}_3)_2(\text{CO})_4$. This transition can be understood from the fact that PET_3 is a donor and CO is an acceptor, so the stability is maximized when donor–acceptor pairs are formed.^{49,50} For the donor rich clusters with more PET_3 than CO ligands, replacing PET_3 with CO is energetically favorable, while, for the species with five or six CO, the replacement with PET_3 is favorable. The maximum stability at $\text{Co}_6\text{Te}_8(\text{PET}_3)_2(\text{CO})_4$ is partially due to the intrinsic binding energy of CO being slightly larger than that of PET_3 , and the fact that the cluster may also serve as an acceptor. In fact, successive substitution of PET_3 with CO for cobalt based chalcogenide clusters in the solution phase has been recently reported by Champsaur et al., and our findings are consistent with their observations.^{29,51} Though the difference in binding strength of ligands is relatively small, we now show that the

substitution strongly affects some of the electronic properties of the clusters. All of the $\text{Co}_6\text{Te}_8(\text{PET}_3)_m(\text{CO})_n$ ($m + n = 6$) clusters are found to have a singlet ground state irrespective of the ligand combination, and all are marked by the large HOMO–LUMO gap ranging from 1.24 to 1.39 eV. **Figure 3**

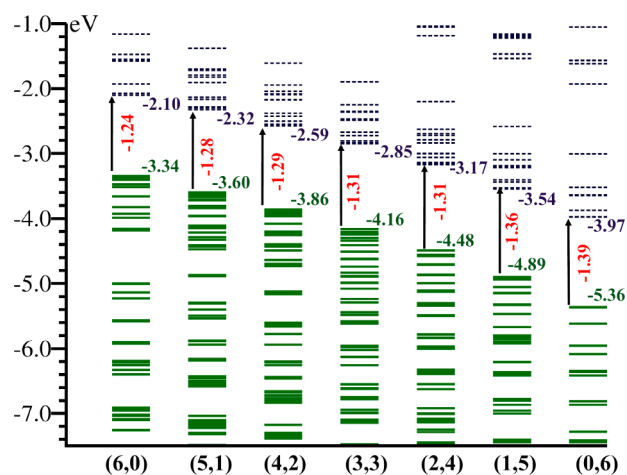


Figure 3. One electron energy levels of ligated $\text{Co}_6\text{Te}_8(\text{PET}_3)_m(\text{CO})_n$ ($m + n = 6$) clusters. Solid and dashed lines represent the occupied and empty energy levels. The values of HOMO, LUMO, and HOMO–LUMO gap are also given.

shows the one-electron energy levels in the optimized ground states of $\text{Co}_6\text{Te}_8(\text{PET}_3)_m(\text{CO})_n$. It is interesting to see that exchange with CO ligands leaves the HOMO–LUMO gap largely unchanged, as shown in **Figure 4a**. The HOMO and LUMO levels, however, are monotonically shifted to deeper energies. As a result, a progressive increase in their AIEs and AEAs shown in **Figure 4b** is observed. All of the values of HOMO, LUMO, AIEs, and AEAs are given in **Table SI-II**. While $\text{Co}_6\text{Te}_8(\text{PET}_3)_6$ has a low ionization energy of 4.75 eV, $\text{Co}_6\text{Te}_8(\text{CO})_6$ has a high AIE of 7.42 eV as well as a high AEA of 2.79 eV. The electron affinity is only slightly less than that of an iodine atom (3.06 eV), a known halogen. The change from alkali to halogen for the same metal core simply by the replacement of ligands is quite intriguing, as all the clusters have filled electronic shells with a large HOMO–LUMO gap. Since the HOMO and LUMO are displaced by electron filling, it is important to ask whether a change in the electron count is the underlying mechanism for the observed trends. In order to examine this, we investigated the partial density of electronic states (PDOS) of all the clusters, as shown in **Figure 5**. Each

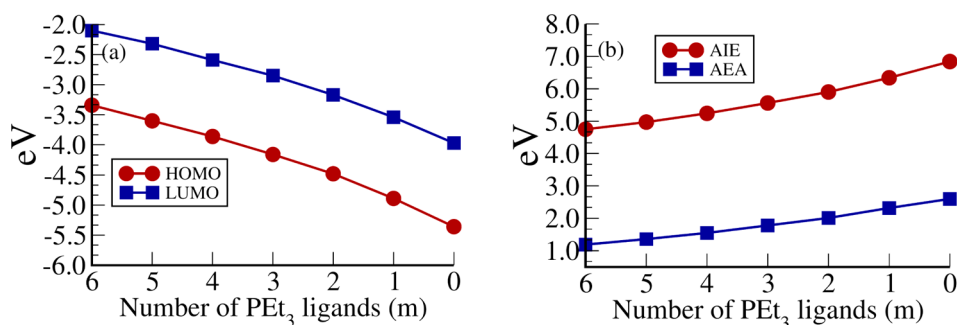


Figure 4. (a) The HOMO and LUMO and (b) the adiabatic ionization energy (AIE) and adiabatic electron affinity (AEA) of $\text{Co}_6\text{Te}_8(\text{PET}_3)_m(\text{CO})_n$ ($m + n = 6$) clusters.

peak in the PDOS corresponding to the energies of molecular orbitals was broadened by a Lorentzian curve of width 0.025 eV to obtain continuous lines. The dotted line indicates the Fermi level or the position of the HOMO of the cluster. The HOMO or LUMO states in all cases are primarily composed of 3d-Co and p-Te states, as in the case of a bare Co_6Te_8 cluster. These states continuously move to lower energy as PET_3 is substituted by CO. Furthermore, the PET_3 and CO derived states always reside either deeper or higher in energy relative to the Fermi level, respectively (**Figure 5**). Consequently, the progressive shift in the AIE and AEA is associated with the position of HOMO and LUMO states derived from the metal core rather than a change in the electron count. To probe how the ligands could affect such changes, the nature of bonding between the ligands and the metal core needs to be highlighted. The phosphine ligands may be expected to form charge transfer complexes, while the CO tends to form covalent bonds. In both cases, the interaction is with the Co 4s orbitals that lie deeper in the electronic structure. We therefore carried out a Hirshfeld charge analysis to examine the net charge on the metal core as the ligands are changed. A local Hirshfeld charge analysis of the optimized Co_6Te_8 shows that each Co atom has an average charge of $-0.14 e^-$ while each Te atom carries $+0.10 e^-$ charge. The addition of the PET_3 ligand on Co_6Te_8 increases the average negative charge on Co and the Te atom becomes less positively charged, resulting in a net charge of $-0.52 e^-$ on the metal core. In the case of $\text{Co}_6\text{Te}_8(\text{CO})_6$, the total charge on the Co atoms is approximately the same as that for the bare Co_6Te_8 cluster, while the Te atoms become more positively charged, thereby leading to a net charge of $+0.31 e^-$ on the core. The values of Hirshfeld charges are given in **Table SI-III**. In addition, the net negative charge on the metal core, starting from the fully ligated PET_3 , monotonically decreases and becomes positive as the PET_3 are substituted by CO. **Figure 6** shows the net charge at the metal core as well as the charge on the PET_3 and CO ligands for $\text{Co}_6\text{Te}_8(\text{PET}_3)_m(\text{CO})_n$ clusters. The PET_3 ligands are donors, so they carry a positive charge, while CO ligands are negatively charged, as they are electron acceptors. In any case, the progression in AIE and AEA seems to be driven by the net charge on the metal core. It is instructive to develop a simple model that could account for the observed trends qualitatively. The ligands undergo covalent bonding but also change the net charge on the cluster.

We therefore proceeded to examine if the change in charged state could provide an idea about the shift. Considering the $\text{Co}_6\text{Te}_8(\text{PET}_3)_6$ cluster, we considered a model where the net charge of $-0.52 e^-$ on the metal core is partitioned into six equal negative fictitious point charges ($-0.087 e^-$) placed

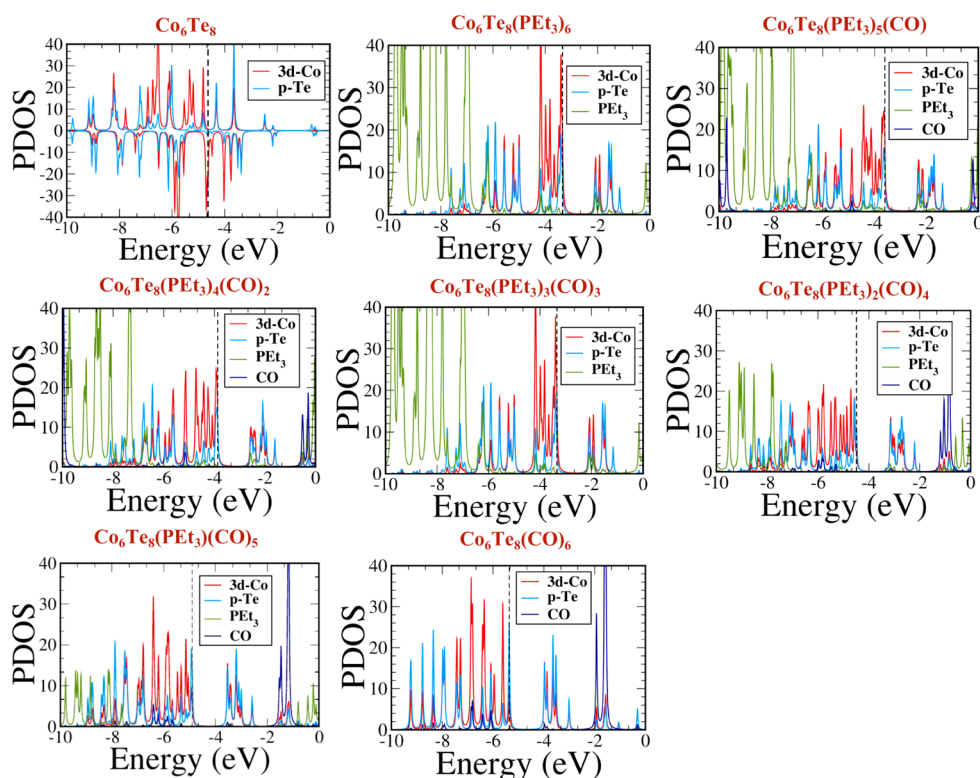


Figure 5. Partial density of states (PDOS) in the optimized ground state structures of a bare Co_6Te_8 and ligated $\text{Co}_6\text{Te}_8(\text{PEt}_3)_m(\text{CO})_n$ ($m + n = 6$) clusters. The orbital energies are widened by Lorentzians with a width of 0.025 eV, and dotted lines indicate the energy of the HOMO. The states corresponding to ligands (PEt_3 and CO) reside deeper and higher in energy relative to the Fermi level.

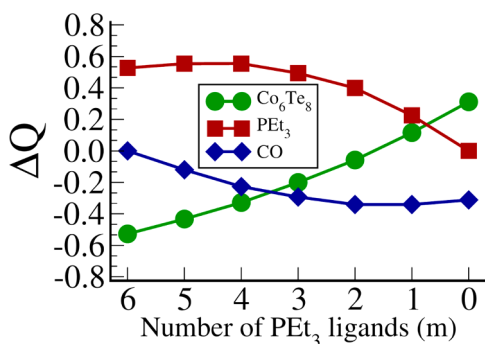


Figure 6. Net charge on Co_6Te_8 , PEt_3 , and CO ligands of $\text{Co}_6\text{Te}_8(\text{PEt}_3)_m(\text{CO})_n$ ($m + n = 6$) clusters.

around 0.5 Å away from the Co sites of the optimized Co_6Te_8 . The fictitious charges were placed close to Co sites, as the Hirshfeld analysis indicated that the Co sites gain the charge. Similarly, the net positive charge on the core in the case of $\text{Co}_6\text{Te}_8(\text{CO})_6$ was partitioned into eight fictitious positive charges and placed around 0.5 Å from the Te sites. The fictitious charges were placed close to Te sites, as the Hirshfeld analysis indicated that the Te sites lose the charge. Figure 7 shows the PDOS for such models. The major effect is a shifting of the electronic spectrum up and down in energy as observed in real systems. The positions of HOMOs are found to be -2.46 and -5.46 eV compared to -4.63 eV of the optimized Co_6Te_8 cluster. As we can see, qualitative progressions are in the correct direction as in the optimized ligated systems but the magnitude of change is different. The above considerations show that the qualitative shifts in the HOMO and LUMO may

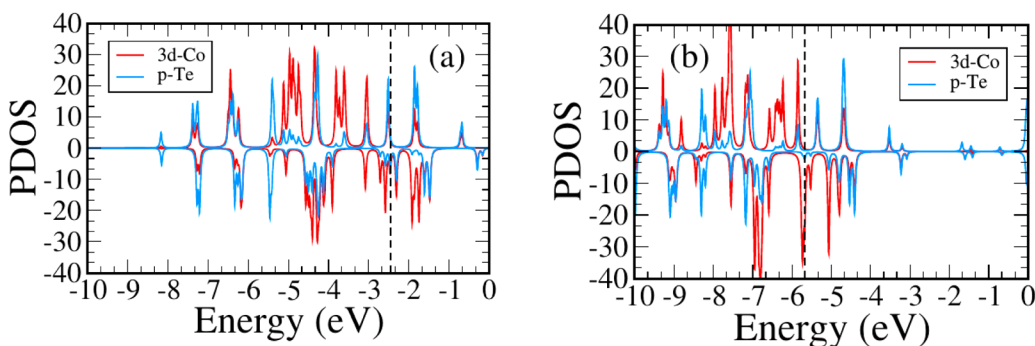


Figure 7. Partial density of states: (a) Co_6Te_8 with negative point charges; (b) Co_6Te_8 with positive point charges. The orbital energies are widened by Lorentzians with a width of 0.025 eV, and dotted lines indicate the energy of the HOMO.

be rationalized within a simple picture where the metal core is embedded in a coulomb well created by the charge transfer in the presence of ligands. It is important to highlight that these considerations are extremely simplistic. Replacing the ligands with fictitious point charges by no means would provide the actual HOMO–LUMO gap and changes in the magnetic character of real systems.

CONCLUSIONS

To summarize, our studies show that $\text{Co}_6\text{Te}_8(\text{PEt}_3)_m(\text{CO})_n$ clusters present an unusual class of stable clusters that are all marked by closed electronic shells with large HOMO–LUMO gaps and yet may offer low ionization energies or high electron affinity depending on the choice of ligand. As we show, these features are not derived from changes in the filling of the electronic shells but rather by the shifting of the electronic spectrum. Consequently, these clusters have the potential to have oxidation states where they can accept or donate multiple electrons from these shells. The ability to manipulate the location of the HOMO or LUMO is critical to applications in photovoltaics. We also show that the progressions of the HOMO or LUMO can be rationalized on the basis of a coulomb well formed by the electron withdrawing and electron donating ligands. Finally, the ground state geometries favor a symmetrical substitution of ligands that could allow formation of cluster molecules or cluster assemblies using appropriate ligands. We hope that the present findings will stimulate further interest in using ligands for controlling the donor–acceptor properties in clusters.

ASSOCIATED CONTENT

Supporting Information

The Supporting Information is available free of charge on the ACS Publications website at DOI: 10.1021/jacs.6b09416.

The optimized Cartesian coordinates of $\text{Co}_6\text{Te}_8(\text{PEt}_3)_m(\text{CO})_n$ and tabulated data on the bond lengths, Hirshfeld charges, HOMO–LUMO gaps, AEs, and AIEs (PDF)

AUTHOR INFORMATION

Corresponding Author

*snkhanna@vcu.edu

ORCID

Shiv N. Khanna: 0000-0002-9797-1289

Notes

The authors declare no competing financial interest.

ACKNOWLEDGMENTS

This material is based upon work supported by the US Department of Energy (DOE) under the award number DE-SC0006420.

REFERENCES

- (1) Khanna, S. N.; Jena, P. *Phys. Rev. B: Condens. Matter Mater. Phys.* **1995**, *51*, 13705.
- (2) Castleman, A. W.; Khanna, S. N. *J. Phys. Chem. C* **2009**, *113*, 2664.
- (3) Knight, W. D.; Clemenger, K.; de Heer, W. A.; Saunders, W. A.; Chou, M. Y.; Cohen, M. L. *Phys. Rev. Lett.* **1984**, *52*, 2141.
- (4) Reber, A. C.; Khanna, S. N.; Roach, P. J.; Woodward, W. H.; Castleman, A. W. *J. Am. Chem. Soc.* **2007**, *129*, 16098.

- (5) Bergeron, D. E.; Castleman, A. W.; Morisato, T.; Khanna, S. N. *Science* **2004**, *304*, 84.
- (6) Bergeron, D. E.; Roach, P. J.; Castleman, A. W.; Jones, N. O.; Khanna, S. N. *Science* **2005**, *307*, 231.
- (7) Reber, A. C.; Khanna, S. N.; Castleman, A. W. *J. Am. Chem. Soc.* **2007**, *129*, 10189.
- (8) Yang, J.; Wang, X.-B.; Xing, X.-P.; Wang, L.-S. *J. Chem. Phys.* **2008**, *128* (20), 201102.
- (9) Li, Y.; Wu, D.; Li, Z.-R. *Inorg. Chem.* **2008**, *47*, 9773.
- (10) Held, A.; Moseler, M.; Walter, M. *Phys. Rev. B: Condens. Matter Mater. Phys.* **2013**, *87*, 045411.
- (11) Jadzinsky, P. D.; Calero, G.; Ackerson, C. J.; Bushnell, D. A.; Kornberg, R. D. *Science* **2007**, *318*, 430.
- (12) Zhu, M.; Aikens, C. M.; Hollander, F. J.; Schatz, G. C.; Jin, R. *J. Am. Chem. Soc.* **2008**, *130*, 5883.
- (13) Akola, J.; Kacprzak, K. A.; Lopez-Acevedo, O.; Walter, M.; Grönbeck, H.; Häkkinen, H. *J. Phys. Chem. C* **2010**, *114*, 15986.
- (14) Bertino, M. F.; Sun, Z.-M.; Zhang, R.; Wang, L.-S. *J. Phys. Chem. B* **2006**, *110*, 21416.
- (15) Biltek, S. R.; Mandal, S.; Sen, A.; Reber, A. C.; Pedicini, A. F.; Khanna, S. N. *J. Am. Chem. Soc.* **2013**, *135*, 26.
- (16) Heaven, M. W.; Dass, A.; White, P. S.; Holt, K. M.; Murray, R. W. *J. Am. Chem. Soc.* **2008**, *130*, 3754.
- (17) Clayborne, P. A.; Lopez-Acevedo, O.; Whetten, R. L.; Grönbeck, H.; Häkkinen, H. *J. Chem. Phys.* **2011**, *135*, 094701.
- (18) Mandal, S.; Reber, A. C.; Qian, M.; Weiss, P. S.; Khanna, S. N.; Sen, A. *Acc. Chem. Res.* **2013**, *46*, 2385.
- (19) George, A.; Asha, K. S.; Reber, A. C.; Biltek, S. R.; Pedicini, A. F.; Sen, A.; Khanna, S. N.; Mandal, S. *Nanoscale* **2015**, *7*, 19448.
- (20) Clayborne, P. A.; Lopez-Acevedo, O.; Whetten, R. L.; Grönbeck, H.; Häkkinen, H. *Eur. J. Inorg. Chem.* **2011**, *2011*, 2649.
- (21) Lopez-Acevedo, O.; Akola, J.; Whetten, R. L.; Grönbeck, H.; Häkkinen, H. *J. Phys. Chem. C* **2009**, *113*, 5035.
- (22) Abreu, M. B.; Powell, C.; Reber, A. C.; Khanna, S. N. *J. Am. Chem. Soc.* **2012**, *134*, 20507.
- (23) Luo, Z.; Reber, A. C.; Jia, M.; Blades, W. H.; Khanna, S. N.; Castleman, A. W. *Chem. Sci.* **2016**, *7*, 3067.
- (24) Walter, M.; Akola, J.; Lopez-Acevedo, O.; Jadzinsky, P. D.; Calero, G.; Ackerson, C. J.; Whetten, R. L.; Grönbeck, H.; Häkkinen, H. *Proc. Natl. Acad. Sci. U. S. A.* **2008**, *105*, 9157.
- (25) Roy, X.; Lee, C.-H.; Crowther, A. C.; Schenck, C. L.; Besara, T.; Lalancette, R. A.; Siegrist, T.; Stephens, P. W.; Brus, L. E.; Kim, P.; Steigerwald, M. L.; Nuckolls, C. *Science* **2013**, *341*, 157.
- (26) Lee, C.-H.; Liu, L.; Bejger, C.; Turkiewicz, A.; Goko, T.; Arguello, C. J.; Frandsen, B. A.; Cheung, S. C.; Medina, T.; Munsie, T. J. S.; D'Ortenzio, R.; Luke, G. M.; Besara, T.; Lalancette, R. A.; Siegrist, T.; Stephens, P. W.; Crowther, A. C.; Brus, L. E.; Matsuo, Y.; Nakamura, E.; Uemura, Y. J.; Kim, P.; Nuckolls, C.; Steigerwald, M. L.; Roy, X. *J. Am. Chem. Soc.* **2014**, *136*, 16926.
- (27) Turkiewicz, A.; Paley, D. W.; Besara, T.; Elbaz, G.; Pinkard, A.; Siegrist, T.; Roy, X. *J. Am. Chem. Soc.* **2014**, *136*, 15873.
- (28) Choi, B.; Yu, J.; Paley, D. W.; Trinh, M. T.; Paley, M. V.; Karch, J. M.; Crowther, A. C.; Lee, C.-H.; Lalancette, R. A.; Zhu, X.; Kim, P.; Steigerwald, M. L.; Nuckolls, C.; Roy, X. *Nano Lett.* **2016**, *16*, 1445.
- (29) Champsaur, A. M.; Velian, A.; Paley, D. W.; Choi, B.; Roy, X.; Steigerwald, M. L.; Nuckolls, C. *Nano Lett.* **2016**, *16*, 5273.
- (30) Yu, J.; Lee, C.-H.; Bouilly, D.; Han, M.; Kim, P.; Steigerwald, M. L.; Roy, X.; Nuckolls, C. *Nano Lett.* **2016**, *16*, 3385.
- (31) Fenske, D.; Hachgenei, J.; Ohmer, J. *Angew. Chem., Int. Ed. Engl.* **1985**, *24*, 706.
- (32) Boardman, B. M.; Widawsky, J. R.; Park, Y. S.; Schenck, C. L.; Venkataraman, L.; Steigerwald, M. L.; Nuckolls, C. *J. Am. Chem. Soc.* **2011**, *133*, 8455.
- (33) Chauhan, V.; Sahoo, S.; Khanna, S. N. *J. Am. Chem. Soc.* **2016**, *138*, 1916.
- (34) Chauhan, V.; Reber, A. C.; Khanna, S. N. *J. Phys. Chem. A* **2016**, *120*, 6644.
- (35) Reeves, B. J.; Boardman, B. M. *Polyhedron* **2014**, *73*, 118.

- (36) Reeves, B. J.; Shircliff, D. M.; Shott, J. L.; Boardman, B. M. *Dalton Trans* **2015**, *44*, 718.
- (37) Kamiguchi, S.; Imoto, H.; Saito, T.; Chihara, T. *Inorg. Chem.* **1998**, *37*, 6852.
- (38) Brunner, H.; Lucas, D.; Monzon, T.; Mugnier, Y.; Nuber, B.; Stubenhofer, B.; Stückl, A. C.; Wachter, J.; Wanninger, R.; Zabel, M. *Chem. - Eur. J.* **2000**, *6*, 493.
- (39) Seidel, R.; Kliss, R.; Weissgräber, S.; Henkel, G. *J. Chem. Soc., Chem. Commun.* **1994**, 2791.
- (40) Gutsev, G. L.; Khanna, S. N.; Rao, B. K.; Jena, P. *Phys. Rev. A: At., Mol., Opt. Phys.* **1999**, *59*, 3681.
- (41) Imahori, H. *J. Mater. Chem.* **2007**, *17*, 31.
- (42) Cho, Y.-J.; Ahn, T. K.; Song, H.; Kim, K. S.; Lee, C. Y.; Seo, W. S.; Lee, K.; Kim, S. K.; Kim, D.; Park, J. T. *J. Am. Chem. Soc.* **2005**, *127*, 2380.
- (43) Wang, D. H.; Park, K. H.; Seo, J. H.; Seifert, J.; Jeon, J. H.; Kim, J. K.; Park, J. H.; Park, O. O.; Heeger, A. J. *Adv. Energy Mater.* **2011**, *1*, 766.
- (44) te Velde, G.; Bickelhaupt, F. M.; Baerends, E. J.; Fonseca Guerra, C.; van Gisbergen, S. J. A.; Snijders, J. G.; Ziegler, T. *J. Comput. Chem.* **2001**, *22*, 931.
- (45) Perdew, J. P.; Burke, K.; Ernzerhof, M. *Phys. Rev. Lett.* **1996**, *77*, 3865.
- (46) van Lenthe, E.; Snijders, J. G.; Baerends, E. J. *J. Chem. Phys.* **1996**, *105*, 6505.
- (47) Steigerwald, M. L.; Siegrist, T.; Stuczynski, S. M. *Inorg. Chem.* **1991**, *30*, 2256.
- (48) Bencini, A.; Fabrizi de Biani, F.; Uytterhoeven, M. G. *Inorg. Chim. Acta* **1996**, *244*, 231.
- (49) Metiu, H.; Chrétien, S.; Hu, Z.; Li, B.; Sun, X. *J. Phys. Chem. C* **2012**, *116*, 10439.
- (50) Reber, A. C.; Khanna, S. N. *J. Phys. Chem. C* **2014**, *118*, 20306.
- (51) Steigerwald, M. L.; Stuczynski, S. M.; Kwon, Y.-U.; Vennos, D. A.; Brennan, J. G. *Inorg. Chim. Acta* **1993**, *212*, 219.